analytical chemistry

Technical Note

pubs.acs.org/ac

Characterization of Polymer Monoliths Containing Embedded Nanoparticles by Scanning Transmission X-ray Microscopy (STXM)

R. Dario Arrua,[†] Adam P. Hitchcock,[‡] Wei Boon Hon,[†] Marcia West,[§] and Emily F. Hilder*[,†]

[†]Australian Centre for Research on Separation Science (ACROSS), School of Chemistry, University of Tasmania, Private Bag 75, Hobart 7001, Australia

[‡]Department of Chemistry and Chemical Biology, McMaster University, Hamilton, ON L8S 4M1, Canada

[§]Faculty of Health Sciences Electron Microscopy Facility, McMaster University, Hamilton, ON L8N 3Z5, Canada

Supporting Information

ABSTRACT: The structural and chemical homogeneity of monolithic columns is a key parameter for high efficiency stationary phases in liquid chromatography. Improved characterization techniques are needed to better understand the polymer morphology and its optimization. Here the analysis of polymer monoliths by scanning transmission X-ray microscopy (STXM) is presented for the first time. Poly(butyl methacrylate-*co*-ethyleneglycoldimethacrylate) [poly(BuMA-*co*-EDMA)] monoliths containing encapsulated divinylbenzene (DVB) nanoparticles were characterized by STXM, which gives a comprehensive, quantitative chemical analysis of the monolith at a spatial resolution of 30 nm. The results are compared with other methods commonly used for the characterization of polymer monoliths [scanning electron microscopy (SEM), transmission electron microscopy (TEM), mercury porosimetry, and nitrogen adsorption]. The technique permitted chemical identification and mapping of the nanoparticles within the polymeric scaffold. Residual surfactant, which was used during the manufacture of the nanoparticles, was also detected. We show that STXM can give more in-depth chemical information for these types of materials and therefore lead to a better understanding of the link between polymer morphology and chromatographic performance.

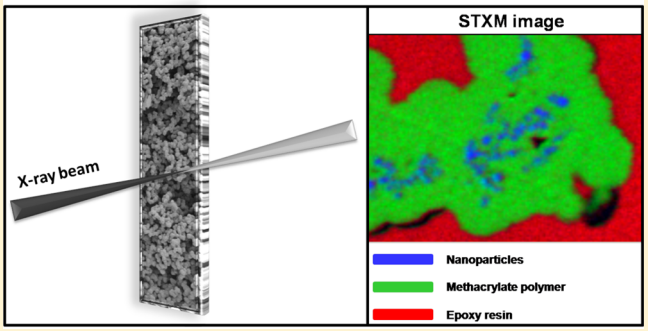

Monolithic polymers were introduced more than 20 years ago[1,2] and have become increasingly popular as a new generation of stationary phase to be used in separation science with recognized advantages over their particulate counterparts. Their best-known advantage is a rigid structure with high permeability due to the presence of large through pores, which permit the use of high liquid flow rates at low backpressures. Generally, they are prepared by free radical initiated polymerization from a homogeneous polymerization mixture, which consists of the mono- and divinyl- monomers, porogenic mixture, and free radical initiator.[3]

Although monolithic columns are a mature column technology with commercially available columns, improvements in this technology are continually sought and these generally rely on being able to perform a comprehensive and accurate characterization of both the morphology and chemistry of the material. The porous structure of monolithic materials is usually examined by scanning electron microscopy (SEM);[3] however, the information obtained with this technique is limited since only the surface morphology of the material is probed. Recently, alternative characterization techniques have been used to gain a more comprehensive understanding of the structural morphology of polymer monoliths. These techniques include transmission electron microscopy (TEM),[4] serial block-face SEM,[5] neutron scattering,[6] and atomic force microscopy (AFM).[7,8] As an example, Müllner et al.[5] demonstrated the radial heterogeneity of the macroporous structure of hyper-cross-linked poly(styrene-*co*-divinylbenzene) monoliths at the microscale level by serial block-face SEM, while Laher et al.[8] characterized the mechanical properties of the polymer globules of commercial styrene- and methacrylate-based monoliths by AFM, demonstrating varying degrees of cross-linking of the polymeric globules. All the characterization techniques mentioned above give information about the structure/mechanical properties of the monolithic materials. However, these methods have certain limitations when performing analysis of the spatial distribution of the different chemical components of the material. Since liquid chromatography is a technique based on the interactions between the surface of the stationary phase and the analytes present in the mobile phase, detailed knowledge of the chemical composition of the materials used as stationary phases would give important complementary insights in regards to the characterization of polymer monoliths.

Received: October 2, 2013
Accepted: February 19, 2014
Published: February 19, 2014

   dx.doi.org/10.1021/ac403166u | *Anal. Chem.* 2014, 86, 2876−2881

In this work, we demonstrate the use of scanning transmission X-ray microscopy (STXM) as a new technique for the characterization of polymer monoliths. STXM is a synchrotron-based technique which combines near edge X-ray absorption fine structure (NEXAFS) spectroscopy and soft X-ray scanning microscopy with a spatial resolution on the order of 30 nm.[9−12] STXM has been used previously for the characterization of different nanocomposite polymeric materials such as microcapsules used as release gates,[13] colloidal photonic crystals,[14] and osmosis membranes.[15]

The application of STXM to the field of liquid chromatography support phases is demonstrated by STXM analysis of poly(butyl methacrylate-*co*-ethyleneglycoldimethacrylate) [poly(BuMA-*co*-EDMA)] monoliths containing embedded divinylbenzene (DVB) nanoparticles. The choice of this material was based on the fact that direct encapsulation of nanostructures within monolithic scaffolds is one of the most recent approaches toward functionalization of these polymer monoliths.[16−21] However, there is a lack of understanding in terms of the effect the nanostructures have on the morphology of the porous materials and the spatial distribution of the nanostructures within the polymer structure. The results are compared to SEM, TEM, and capillary liquid chromatography on these materials and in some cases on exactly the same microtomed section studied by STXM.

EXPERIMENTAL SECTION

Reagents and Materials. Butyl methacrylate (BuMA) (99%), ethylene glycol dimethacrylate (EDMA) (98%,), divinylbenzene (DVB, 80%), hexadecane (HD), sodium dodecilsulfate (SDS), 1-propanol (99%), 1,4-butanediol (99%), 2,2-dimethoxy-2-phenylacetophenone DMPA (99%), 3-(trimethoxysilyl)propyl methacrylate (98%), trimethylolpropanetriglycidyl ether (TTE), and 4,4′-methylenebis (2-methylcyclohexylamine) (MMCA) were purchased from Aldrich (Milwaukee, WI). BuMA, EDMA, and DVB were passed through a bed of basic alumina (50−55% Aldrich) to remove inhibitors. All other reagents were of the highest available grade and were used as received. Water used in all experiments was purified by a Milli-Q system (Millipore, Milford, MA). The Teflon-coated UV transparent fused-silica capillary (100 μm i.d.) was obtained from Polymicro Technologies Inc. (Phoenix, AZ).

Instrumentation. An OAI deep UV illumination system (model LS30/5, San Jose, CA) fitted with a 500 W HgXe lamp was used for the UV-initiated polymerization reactions. For calibration, the irradiation power was adjusted to 20.0 mW/cm^2, using an OAI model 206 intensity meter with a 260 nm probe head. The porous properties of the bulk polymers were characterized by specific surface area, as determined by the Brunauer−Emmet−Teller method[22] and mercury intrusion porosimetry studies. BET analysis was performed with a micromeritics ASAP 2400 BET Surface Area Analyzer (Norcross, GA) and porosimetry studies were carried out using a Micromeritics Pore Sizer 9310. Dynamic light scattering measurements of the nanoparticles were performed on a Malvern Instruments, Zetasizer Nano-ZS (Worcestershire, U.K.).

The surface morphology of each of the different monoliths prepared in this work was analyzed by SEM, using a FEI Quanta 600 MLA ESEM in the Central Science Laboratory, University of Tasmania. The capillaries were sputter-coated with platinum. Bright field TEM images were obtained at the McMaster Faculty of Health Sciences electron microscopy facility using a JEOL 1200EX operating at 80 kV. STXM measurements were performed using the STXM at the 10ID1 beamline at the Canadian Light Source (CLS, Saskatoon, SK, Canada). The STXM measurements in this case required ∼2 h of beamtime and a further 2 h of data analysis.

To prepare samples for TEM and STXM analysis, the polymer monolith containing DVB nanoparticles was embedded with an aliphatic epoxy resin consisting of a 1:1 mixture of trimethylolpropane triglycidyl ether (TTE) and an alicyclic amine, 4,4′-methylene bis (2-methylcyclohexylamine) (MMCA), and was cured overnight at 60 °C. The embedded sample was then ultramicrotomed at room temperature into ∼100 nm thin sections which were floated on distilled water and picked up onto Formvar-coated 100 mesh Cu TEM grids (see Figure S1 of the Supporting Information).

Synthesis of PolyDVB Nanoparticles. Nanoparticles of DVB were prepared by mini-emulsion polymerization using a procedure previously reported.[18] Briefly, 6.0 g of monomer (DVB), 0.26 g of HD, and 0.06 g of AIBN were added slowly to an aqueous phase composed of 283.5 g of H_2O and 0.23 g of SDS. This mixture was emulsified by ultrasonication (450 Branson Digital Sonifier) in an ice bath at 70% amplitude for 6.5 min in 1 min intervals with a 30 s rest. The mini-emulsion was placed in a three-neck flask and deoxygenated with nitrogen for 15 min. Finally, the polymerization reaction was carried out in an oil bath at 65 °C for 16 h. The latex nanoparticles obtained were purified by membrane dialysis for 48 h, changing the water every 5 h. The polymerization yield and solid content were determined by gravimetry. The size of the nanoparticles, as determined by dynamic light scattering, was around 187 nm.

Preparation of Porous Polymer Monoliths. The monoliths characterized in this study were prepared in both capillary and bulk format. For the preparation of the capillary column, the surface of Teflon-coated fused-silica capillaries were modified with 3-(trimethoxysilyl)propyl methacrylate using a procedure previously described.[18] A polymerization mixture consisting of 0.4 g (16 wt %) BuMA, 0.6 g (24 wt %) EDMA, 0.15 g (6 wt %) water, 0.3 g (12 wt %) 1,4-butanediol, 1.05 g (42 wt %) 1-propanol, and 10 mg DMPA (1 wt % with respect to monomers) was prepared and deoxygenated with nitrogen for 10 min. A surface-modified capillary was then filled with the polymerization mixture, and irradiated with UV light for 10 min. After photopolymerization, the column was washed with methanol at 30 μL/min for 3 h to remove the porogen and any unreacted monomers. A similar procedure was used for the preparation of the poly(BuMA-*co*-EDMA) monolith containing DVB nanoparticles. In this case, water was replaced in the polymerization mixture by 0.15 g of a 4.65 wt % aqueous suspension of DVB nanoparticles. For the preparation of bulk polymer, a special cast was designed (Figure S2 of the Supporting Information). A piece of Teflon (500 μm thick) was used to form a Teflon rim along the edges of a 76 × 51 mm, 1 mm thickness glass slide (ProSciTech, Thuringowa, Qld, Australia). The Teflon rim was glued to the glass slide using an epoxy adhesive (Araldite 5 minute Everyday, Shelley Pty. Ltd. New South Wales, Australia). The polymerization mixture was transferred into the cast using a Pasteur pipet. The cast was then covered with a clean glass slide and clamped with bulldog clips as shown in Figure S2 of the Supporting Information. With the solution in place and the two halves of the glass slides secured, the container was then irradiated with UV light for 15

dx.doi.org/10.1021/ac403166u | *Anal. Chem.* 2014, 86, 2876−2881

min. The prepared polymer was removed from the cast and the material was extracted with methanol using a Soxhlet apparatus for 12 h, before being vacuum-dried at 60 °C for a further 12 h. These materials were later used for mercury intrusion porosimetry and specific surface area analysis.

RESULTS AND DISCUSSION

One of the more recent approaches to incorporate functionality into polymer monoliths is through the incorporation of nanoparticles, with direct encapsulation as one synthetic strategy. Although it has been demonstrated that better chromatographic separations can be achieved through the encapsulation of nanoparticles within the polymeric structure,[16−20] the 3D spatial distribution of the nanoparticles within the monolithic columns is still not clear. As an example, Krenkova et al.[20] reported the entrapment of hydroxyapatite nanoparticles within poly(2-hydroxyethyl methacrylate-*co*-ethylene dimethacrylate) monoliths and the authors hypothesized that the nanoparticles were entrapped underneath the polymer structure. However, in that work, it was not possible to confirm the exact location of the nanoparticles by SEM and energy dispersive X-ray (EDX) analyses. In this work, poly(BuMA-*co*-EDMA) with encapsulated DVB nanoparticles was prepared as a model polymer monolith. The choice of poly(BuMA-*co*-EDMA) as a polymeric scaffold was based on its recognized hydrophobicity, which permits its use as a stationary phase under the reversed-phase mode. At the same time, the hydrophobic DVB nanoparticles were encapsulated within the poly(BuMA-*co*-EDMA) scaffold in order to modify the porous properties of the material (specific surface, median pore size, pore size distribution, etc.) as well as its surface chemistry (more hydrophobic surface). The monoliths prepared in this work were characterized by STXM as well as commonly used methods in order to demonstrate the complementarity of STXM with other characterization methods.

Monoliths Characterization by Conventional Techniques. The porous properties of poly(BuMA-*co*-EDMA) with and without DVB nanoparticles were determined, and the results obtained are shown in Table 1 (see Figure S3 of the Supporting Information). Table 1 clearly shows that there were no appreciable changes between the specific surface area values for the material with or without the DVB nanoparticles, where the polymer containing DVB nanoparticles presented a slightly higher specific surface area (2.5 ± 0.3 versus 1.7 ± 0.3 m^2/g). The low specific surface area value achieved is contrary to what is expected by incorporating nanostructures into the polymeric scaffold. This suggests that most of the nanoparticles are entrapped within the polymeric scaffold. Similar results were observed for other polymer-based monoliths, where the incorporation of nanostructures did not lead to significant increases in the specific surface area of the materials.[16−18,21] In terms of the porous properties, the pore size distributions obtained (Figure S3 of the Supporting Information) showed that the incorporation of nanoparticles had limited effect on the median pore size and the pore size distribution of the materials prepared.

Table 1. Porous Properties of Poly(BuMA-*co*-EDMA) with and without DVB Nanoparticles

monolith	specific surface area (BET) (m^2/g)	median pore diameter (nm)	total intrusion volume (mL/g)	porosity (%)
poly(BuMA-*co*-EDMA)	1.67 ± 0.28	2032 ± 76	1.63 ± 0.07	59 ± 5
poly(BuMA-*co*-EDMA) + DVB np's	2.45 ± 0.29	2233 ± 75	1.59 ± 0.03	62 ± 3

Scanning electron microscopy (SEM) is commonly used for characterizing stationary phases, giving information about the surface morphology of the materials. SEM analysis of poly(BuMA-*co*-EDMA) control and poly(BuMA-*co*-EDMA) with encapsulated DVB nanoparticles showed almost identical surface morphology, and it was not possible to observe the presence of nanoparticles on the polymer surface (Figure S4 of the Supporting Information). It is also important to mention that, relative to the polymer monolith, the DVB nanoparticles do not have any characteristic atoms which could be used for X-ray fluorescence detection using energy dispersive X-ray spectrometry (EDX), and thus SEM-EDX has significant limitations for characterization of these types of materials.

Another less common characterization technique for monolithic materials is transmission electron microscopy (TEM). This technique gives information about the inner cross-sectional area of the monolith as demonstrated by Courtois et al.[4] TEM images of the poly(BuMA-*co*-EDMA) monolith with encapsulated DVB nanoparticles are shown in Figure S5 of the Supporting Information. The observed dark spots could potentially be the DVB nanoparticles which appear to be fully encapsulated within the polymeric scaffold, and these results could explain the slight differences observed in the porous properties (pore size distribution and specific surface area) of both monoliths. It is worth mentioning that the limitations of TEM-EDX are the same as for SEM-EDX, and thus, it was not possible to perform chemical analysis to confirm that the dark spots were the actual DVB nanoparticles. Electron energy loss spectroscopy in TEM (TEM-EELS) at the C 1s edge could in principle make a specific chemical identification but this analytical method was not available in the TEM used for this study. In addition, the poly(BuMA-*co*-EDMA) material is highly radiation sensitive and would likely be chemically modified by the larger doses needed for TEM-EELS relative to imaging. Quantitative studies of the radiation damage rates for polymethylmethacrylate (PMMA)[23] and polyethylene terephthalate (PET)[24,25] (and many other materials) have shown that, based on acquiring C 1s spectra for chemical analysis, there is a 100−1000 fold advantage (in terms of signal/unit damage) for STXM relative to TEM-EELS.

Monoliths Characterization by Scanning Transmission X-ray Microscopy (STXM). While electron-based microscopy techniques such as SEM and TEM provide excellent nanoscale spatial resolution, their capabilities to give information about the chemical composition and distribution of the sample is limited. In this work, we present the use of scanning transmission X-ray spectromicroscopy (STXM) for the characterization of polymer-based monoliths containing encapsulated DVB nanoparticles. To obtain a suitable sample for STXM studies, the macroporous poly(BuMA-*co*-EDMA) monolith with encapsulated DVB nanoparticles was embedded with an aliphatic epoxy resin specially designed for STXM analysis[26] (see Figure S1 of the Supporting Information). In comparison with other electron-based microscopy techniques recently used for the characterization of polymer-monoliths,[4,5] the sample preparation for STXM does not require staining of the polymer skeleton with heavy metals to increase contrast

dx.doi.org/10.1021/ac403166u | *Anal. Chem.* 2014, 86, 2876−2881

during imaging. Figure 1 shows the C 1s NEXAFS spectra for the different components present in the sample. These spectra

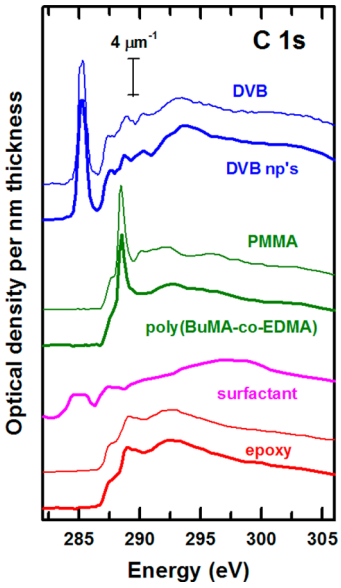

Figure 1. NEXAFS spectra of the methacrylate scaffold (green, compared to that of PMMA), the DVB nanoparticles (blue, compared to that of pure DVB[13]), the TTE epoxy resin (red, compared to that of a different TTE resin sample), and the surfactant (pink). The intensity scales of each spectrum are quantitative (OD/nm) and offsets are used for clarity. The thin traces are the spectra of the pure reference materials.

were extracted from the STXM sample in areas where each component was the only (resin, monolith) or a majority constituent (DVB, surfactant). In the latter case, the overlapping signal from the monolith was subtracted, using comparison to the spectra of pure materials as a guide to the spectral decomposition. Reference spectra of pure materials with similar chemistry are also plotted in Figure 1. The components found by STXM were the poly(BuMA-*co*-EDMA) methacrylate-based polymer scaffold, the DVB nanoparticles, the embedding resin, and a surfactant. The spectrum for the methacrylate scaffold has a strong peak at 288.9 eV, which is characteristic of C 1s → $\pi^*_{C=O}$ transition in esters.[27] The DVB nanoparticles spectrum shows a peak at 285.2 eV, which corresponds to the C 1s → $\pi^*_{C=C}$ transition of the phenyl ring. The C 1s spectrum of the epoxy resin has little or no absorption at these energies and therefore there is excellent contrast between the resin, the scaffold, and the DVB nanoparticles. The spectrum of the surfactant, which was obtained from a very narrow band around the DVB nanoparticles, is again distinct from the other three components. It was initially not included in the analysis of the STXM data but was easily identified from the high residuals in the fit to those pixels with high surfactant content.

These spectroscopic differences allowed identification and mapping of each component of the monolith, which was not possible by SEM or TEM. Figure 2 presents STXM optical density (OD) images at two different energies which were selected for strong chemical contrast. It is possible to see the DVB nanoparticles only at 285.2 eV (Figure 2, panels b and d), while the methacrylate-based scaffold is observed at 288.9 eV (Figure 2, panels c and e). Figure 2f presents a color-coded composite which indicates the spatial relationship of the DVB

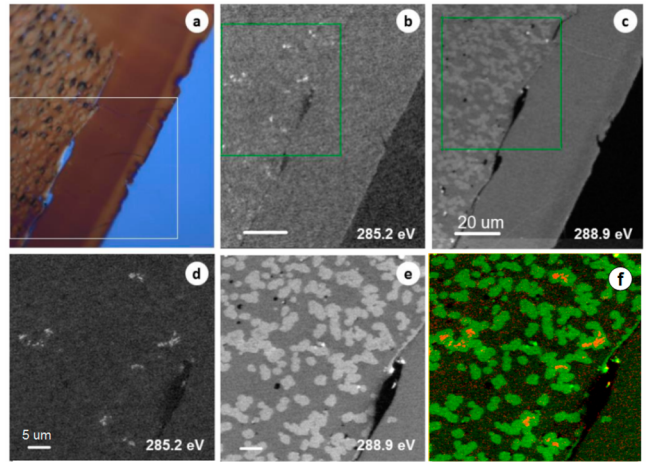

Figure 2. (a) Optical microscopy image of the microtomed section of poly(BuMA-*co*-EDMA) monolith containing DVB nanoparticles. (a) The white rectangle indicates the area where the C 1s images for (b and c) were recorded. STXM optical density (OD) images at (b) 285.2 (π^*_{ring}) and (c) 288.9 eV ($\pi^*_{C=O}$). The green rectangles show the area which has been magnified in (d and e). (f) Color-coded composite map of the (d and e) images (after clipping to expand contrast) with the DVB nanoparticles in red and the methacrylate scaffold in green.

nanoparticles to the monolith. The STXM imaging clearly shows that the nanoparticles are fully embedded within the polymer globules. This observation is in agreement with the results discussed above using conventional characterization techniques (nitrogen adsorption, Hg intrusion porosimetry, SEM, and TEM). It is also possible to see that the nanoparticles are heterogeneously distributed within the sample region analyzed, with a small percentage of the polymer globules having encapsulated DVB nanoparticles.

Figure 3 presents individual component maps of the four chemical species found in the sample. These are derived by

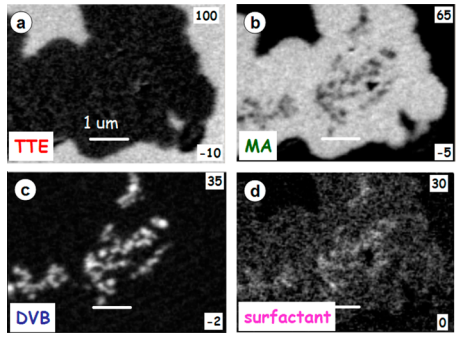

Figure 3. Quantitative component maps of (a) epoxy resin, (b) methacrylate-based scaffold, (c) DVB nanoparticles, and (d) surfactant derived from SVD analysis of a C 1s image sequence. The numbers in the lower and upper right of each panel are thickness scales in nanometers.

singular value decomposition (SVD) analysis[28] (essentially a curve fit of the spectrum at each pixel) of a C 1s image sequence (36 images from 283 to 290 eV), recorded in a small area (6 μm × 4 μm) with a 40 nm pixel spacing to provide a more detailed analysis. Figure 4 shows color-coded composite maps at two different spatial scales (the component maps for Figure 4 (panels a and b) are presented as Figure S-6 of the

dx.doi.org/10.1021/ac403166u | *Anal. Chem.* 2014, 86, 2876−2881

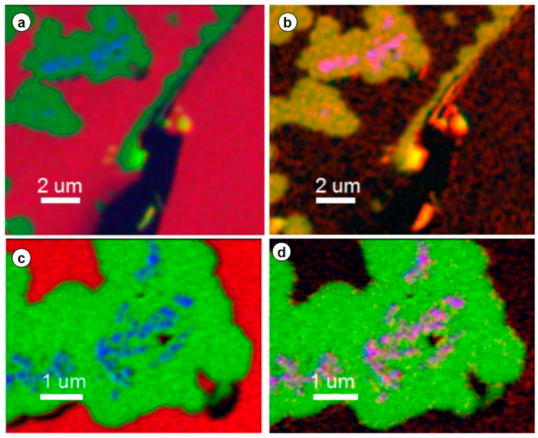

Figure 4. Color-coded composite maps of DVB nanoparticles (blue), methacrylate scaffold (green), epoxy resin (red), and remanent surfactant (pink) (a and b) larger scale and (c and d) expanded scale. The individual component maps for (a and b) are presented in Figure S-7 of the Supporting Information, while Figure 3 provides the component maps for (c and d).

Supporting Information). These color-coded composites display the spatial distribution of the chemical components relative to each other. Again, in both measurements, it can be seen clearly that the DVB nanoparticles are fully embedded within the poly(BuMA-*co*-EDMA) scaffold and therefore they are not available for interaction with the analytes present in the mobile phase when used for chromatographic purposes.

Interestingly, the STXM analysis allowed identification of residual surfactant within the polymer globule (Figure 3d), whose distribution within the polymer globule was extended even beyond the DVB nanoparticles, indicating the surfactant was soluble in the polymerizing poly(BuMA-*co*-EDMA) matrix. The residual surfactant is sodium dodecyl sulfate (SDS), which was used during the synthesis of the DVB nanoparticles. This was an unexpected result. It is now clear that the presence of undesired nanoparticle stabilizers in polymer structures is a real possibility for these materials when these types of nanostructured compounds are used to functionalize a stationary phase in this way. Their presence may in fact lead to undesired secondary interactions, so their detection is extremely important.

The results shown in this work clearly demonstrate how STXM analysis can give detailed chemical information for these materials. This information, in particular the chemical maps, is difficult or impossible (due to radiation damage) to obtain with conventional electron-based techniques, demonstrating the complementarity of STXM with other commonly used methods for the characterization of polymer monoliths.

CONCLUSIONS

In this work, the application of STXM as a new characterization technique for polymer-based stationary phases has been presented. By using this technique, it is possible to obtain information about the spatial distribution of the chemical components of the material, which has not been achieved previously with other conventional electron-based techniques. In terms of the accessibility to STXM, specialized synchrotron facilities are needed, which might limit the application of the technique by other researchers in the field. However, there are a number of STXM beamlines currently worldwide and the opening of new facilities around the world in the near future will provide increased capacity and, thus, improved access to a larger user community.[29] Together with other characterization techniques, the information obtained by STXM can potentially be used to guide improvements to polymer monoliths which are more homogeneous in nature. A polymer monolith containing encapsulated nanoparticles was chosen as a "model" material, and it was found that the particles were fully embedded within the polymer globules, which was in agreement with results deduced using conventional techniques. Even though the application of STXM was only demonstrated in polymer monoliths, it is believed that this method can be applied to a wide range of stationary phases. Current studies in our research group are focused on the exploration of alternative synthetic strategies to improve both the amount of nanoparticles and to achieve an improved distribution within the polymeric scaffold, one where most of the nanoparticles are located at the surface of the polymer globules rather than in the middle of them. Future studies will use STXM to study polymer monoliths containing nanoparticles with different functionalities (for applications in mixed mode chromatography) and polymer monoliths in the solvated state, which cannot be performed with conventional techniques.

ASSOCIATED CONTENT

Supporting Information

Additional information as noted in text. This material is available free of charge via the Internet at http://pubs.acs.org.

AUTHOR INFORMATION

Corresponding Author

*E-mail: Emily.Hilder@utas.edu.au. Tel: +61-3-6226 7670. Fax: +61-3-6226 2858.

Notes

The authors declare no competing financial interest.

ACKNOWLEDGMENTS

This work was supported by the Australian Research Council's Discovery funding scheme (Grant DP0987318). E.F.H. is the recipient of an ARC Future Fellowship (Grant FT0990521). We gratefully acknowledge Dr. Karsten Gömann and Dr. Sandrin Feig (Central Science Laboratory, University of Tasmania) for assistance with scanning electron microscopy. STXM was performed at the Canadian Light Source (CLS) beamline 10ID1. The CLS is supported by CFI, NSERC, CIHR, NRC, and the University of Saskatchewan.

REFERENCES

(1) Svec, F.; Fréchet, J. M. J. *Anal. Chem.* **1992**, *64*, 820−822.
(2) Svec, F.; Fréchet, J. M. J. *Science* **1996**, *273*, 205−211.
(3) Arrua, R. D.; Causon, T. J.; Hilder, E. F. *Analyst* **2012**, *137*, 5179−5189.
(4) Courtois, J.; Szumski, M.; Georgsson, F.; Irgum, K. *Anal. Chem.* **2007**, *79*, 335−344.
(5) Müllner, T.; Zankel, A.; Mayrhofer, C.; Reingruber, H.; Höltzel, A.; Lv, Y.; Svec, F.; Tallarek, U. *Langmuir* **2012**, *28*, 16733−16737.
(6) Ford, K. M.; Konzman, B. G.; Rubinson, J. F. *Anal. Chem.* **2011**, *83*, 9201−9205.
(7) Cabral, J. L.; Bandilla, D.; Skinner, C. D. *J. Chromatogr., A* **2006**, *1108*, 83−89.
(8) Laher, M.; Causon, T. J.; Buchberger, W.; Hild, S.; Nischang, I. *Anal. Chem.* **2013**, *85*, 5645−5649.
(9) Hitchcock, A. P.; Stover, H. D. H.; Croll, L. M.; Childs, R. F. *Aust. J. Chem.* **2005**, *58*, 423−432.
(10) Ade, H.; Hitchcock, A. P. *Polymer* **2008**, *49*, 643−675.

(11) Hitchcock, A. P. In *Handbook of Nanoscopy*; Van Tendeloo, G.; Van Dyck, D.; Pennycook, S. J., Eds.; Wiley-VCH: Weinheim, Germany, 2012, pp 745−791.
(12) Howells, M.; Jacobsen, C.; Warwick, T.; Bos, A. In *Science of Microscopy*, Hawkes, P.; Spence, J. H., Eds.; Springer: New York, 2007, pp 835−926.
(13) Croll, L. M.; Stover, H. D. H.; Hitchcock, A. P. *Macromolecules* **2005**, *38*, 2903−2910.
(14) Hilhorst, J.; Van Schooneveld, M. M.; Wang, J.; De Smit, E.; Tyliszczak, T.; Raabe, J.; Hitchcock, A. P.; Obst, M.; De Groot, F. M. F.; Petukhov, A. V. *Langmuir* **2012**, *28*, 3614−3620.
(15) Mitchell, G. E.; Mickols, B.; Hernandez-Cruz, D.; Hitchcock, A. *Polymer* **2011**, *52*, 3956−3962.
(16) Aqel, A.; Yusuf, K.; Al-Othman, Z. A.; Badjah-Hadj-Ahmed, A. Y.; Alwarthan, A. A. *Analyst* **2012**, *137*, 4309−4317.
(17) Chambers, S. D.; Svec, F.; Fréchet, J. M. J. *J. Chromatogr., A* **2011**, *1218*, 2546−2552.
(18) Arrua, R. D.; Nordborg, A.; Haddad, P. R.; Hilder, E. F. *J. Chromatogr., A* **2013**, *1273*, 26−33.
(19) Huang, H. Y.; Lin, C. L.; Wu, C. Y.; Cheng, Y. J.; Lin, C. H. *Anal. Chim. Acta* **2013**, *779*, 96−103.
(20) Krenkova, J.; Lacher, N. A.; Svec, F. *Anal. Chem.* **2010**, *82*, 8335−8341.
(21) Lei, W.; Zhang, L. Y.; Wan, L.; Shi, B. F.; Wang, Y. Q.; Zhang, W. B. *J. Chromatogr., A* **2012**, *1239*, 64−71.
(22) Brunauer, S.; Emmett, P. H.; Teller, E. *J. Am. Chem. Soc.* **1938**, *60*, 309−319.
(23) Wang, J.; Morin, C.; Li, L.; Hitchcock, A. P.; Scholl, A.; Doran, A. *J. Electron Spectrosc. Relat. Phenom.* **2009**, *170*, 25−36.
(24) Rightor, E. G.; Hitchcock, A. P.; Ade, H.; Leapman, R. D.; Urquhart, S. G.; Smith, A. P.; Mitchell, G.; Fischer, D.; Shin, H. J.; Warwick, T. *J. Phys. Chem. B* **1997**, *101*, 1950−1960.
(25) Wang, J.; Button, G. A.; West, M. M.; Hitchcock, A. P. *J. Phys. Chem. B* **2009**, *113*, 1869−1876.
(26) Hitchcock, A. P.; Li, J.; Reijerkerk, S.; Foley, P.; Stover, H. D. H.; Shirley, I. *J. Electron Spectrosc. Relat. Phenom.* **2007**, *156*, 467−471.
(27) Urquhart, S. G.; Ade, H. *J. Phys. Chem. B* **2002**, *106*, 8531−8538.
(28) Koprinarov, I. N.; Hitchcock, A. P.; McCrory, C. T.; Childs, R. F. *J. Phys. Chem. B* **2002**, *106*, 5358−5364.
(29) Watts, B.; Ade, H. *Mater. Today* **2012**, *15*, 148−157.